*promoting access to White Rose research papers*

White Rose
Research Online

**Universities of Leeds, Sheffield and York**
**http://eprints.whiterose.ac.uk/**

This is an author produced version of a paper published in **Wear.**

White Rose Research Online URL for this paper:
http://eprints.whiterose.ac.uk/3600/

**Published paper**
Lewis, R., Yoxall, A., Marshall, M.B. and Canty, L.A. (2007) *Characterising pressure and bruising in apple fruit,* Wear, Volume 264 (1-2), 37 - 46.

*White Rose Research Online*
*eprints@whiterose.ac.uk*

# CHARACTERISING PRESSURE AND BRUISING IN APPLE FRUIT

R. LEWIS*, A. YOXALL, M.B. MARSHALL, L.A. CANTY

Department of Mechanical Engineering, The University of Sheffield, Mappin Street,

Sheffield, S1 3JD

*Corresponding author

Tel. +44 (0) 114 2227838; Fax. +44 (0) 114 2227890

roger.lewis@sheffield.ac.uk

## ABSTRACT

A large percentage of apples are wasted each year due to damage such as bruising. The apple journey from orchard to supermarket is very complex and apples are subjected to a variety of static and dynamic loads that could result in this damage occurring. The aim of this work was to use a novel ultrasonic technique to study apple contact areas and stresses under static loading that may occur, for example, in bulk storage bins used during harvesting. These results were used to identify load thresholds above which unacceptable damage occurs. They were also used to validate output from a finite element model, which will ultimately be developed into a packaging design tool to help reduce the likelihood of apple damage occurring.

**Keywords:** Apple Contact, Apple Bruising, Ultrasound, Finite Elements

## INTRODUCTION

Apples experience a very complex journey from the tree in an orchard to the supermarket shelf (as shown in Figure 1). At various stages on this journey they undergo a number of processes, including harvesting, packing, sorting, storage and transport. During these processes the apples experience a variety of loading conditions, the two main types being static and dynamic, which possibly cause damage. The dynamic loading may be a single impact, which may occur during harvesting as they are dropped into the picking buckets, or a vibration, which could occur during transportation. The typical static loads and drop heights, where known, are shown in Table 1. This data was obtained both from direct measurements of harvesting and sorting equipment and from previously published literature.

Peggie [2] found that 8-10% of apples were wasted each year and the major cause of this wastage has been identified as being bruising [3], which is generally defined as damage to and discolouration of apple flesh, usually with no breach of the skin [4] (a visible bruise threshold of $100mm^2$ is a typical value used in industry for determining which apples should be discarded due to damage (referred to in [5] and [6])). More recent data from apple distributors, however, has shown that the wastage figure could be 50% or higher. This represents a large cost, not only borne by various parties involved in the journey of the apple from orchard to supermarket, but also by the supermarket, as a significant number of apples are damaged in store (for example, while being put out on display).

The physical loads that a fruit experiences have their primary consequences on the membrane systems of individual cells, which make up the apple flesh [4] (see Figure 2). An important role of the membranes is to keep the liquid constituents separate. When a plant part experiences physical injury its membranes are damaged and are no longer able to do this. As a result, damage can allow the mixing of enzymes from the cytoplasm with molecules (called phenolics) from the vacuole and the resulting reaction causes the brown coloration associated with a bruise.

Many studies of apple bruising have been carried out using a variety of techniques, such as compression and drop tests with apples to study bruise formation [6-9]. Dynamic tests have also been undertaken with instrumented spheres to determine loads during apple sorting [5]. Results, however, are very difficult to interpret and compare, and are of little use to apple distributors or sellers in reducing losses due to bruising. This work is part of a wider project aimed at providing such information in a user-friendlier format.

The aim of the work outlined here was to use a novel non-invasive ultrasonic technique to study static apple contacts, as experienced, for example, during storage in bulk bins, to determine the area of contact and interfacial pressure. The nature of the resulting bruising was also examined in order to find load thresholds at which unacceptable damage occurs. The ultrasonic results were then used to validate the output from a Finite Element (FE) model of an apple, which will ultimately be used as a design tool for improving apple packaging and reducing waste.

## BACKGROUND

### Apple Contact Area Measurement

Previous attempts at measuring fruit contact areas and pressures have used a variety of techniques. Hertz contact analysis has been applied to study orange contacts [10]. This however, has limitations due the assumptions made in its derivation, especially for materials as complex as fruit flesh.

Herold et al. [9] used a commercial tactile sensing system to study ‘Jonica’ apple contacts. This consists of a thin flexible plastic film containing a grid of sensitive material. This had disadvantages, which limited the accuracy of the results. It is an invasive technique, so the measurement system affected the contact conditions and it proved impossible to calibrate the results to obtain actual contact pressures, so no actual pressure data or contact area was presented. Load thresholds were identified, however. These occurred at around 40 and 100N. At these points dips were observed in the force-time plots presented. Despite the deficiencies (affecting the contact and the lack of calibration) this technique is actually used by distributors to look at relative loads in their apple containers.

Rabelo et al. [10] used a board of micro-switches 0.5mm apart to measure areas in orange contacts. These were compared with measurements for rubber spheres and validated with rubber sphere contacts observed through an acrylic plate. Apart from the fact this technique was invasive, it was also relatively crude with low resolution.

The ultrasonic technique, which has been used to study a number of machine element contacts [11-13], has several advantages over the techniques outlined above. It is non-invasive and so will not affect the contact and it is possible to calibrate the results to obtain contact pressures.

## Apple Finite Element Analysis

Finite Element (FE) techniques have been used previously to investigate modes of vibration in apples [14] and to study transient responses of apples to impulse excitations to determine factors influencing sonic measurements [15]. These are used to ascertain apple firmness, which is a good indication of how ripe an apple is. No work has been reported using FE to investigate contact stress and areas.

In the initial study different properties were assigned to each region of the apple (skin, flesh and core), as shown in Table 2. The magnitude of Young’s modulus and Poisson’s ratio used was found to significantly affect the natural frequencies of vibration. In the second FE study, isotropic elastic properties (of the flesh) were assumed. It was not clear, how the different modelling approaches affected the results as little validation was carried out on either. In the second study validation of the modelling approach was carried out by simulating the response of a rubber ball and comparing with experimental results for which there was only limited correlation.

The properties shown in Table 2 were taken from tests using actual apples carried out by Abbott & Lu [16] and Mohsenin [17]. These indicated that the elastic properties of the apple flesh varied according to load orientation and position in the apple (flesh data in Table 2 has been averaged). Failure stresses were also determined for the flesh and these also varied with position in the apple. Typical values were around 0.40-0.51MPa, although, as with all properties, these varied with the relative ripeness of the apples. The greatest failure stresses were found for *medium* ripe apples (levels of relative *ripeness* were based on harvest time and appearance).

In both studies described above a simplified shape was assumed for an apple (see Figure 3). These were created using the four parameter model of Mustafa & Stout [18]. One half of the cross-section is an incomplete ellipse, which is described by the following equation:

$$a^2\left[r\cos\varphi - y\sin\varphi - c\right]^2 + b^2\left[y\cos\varphi + r\sin\varphi\right]^2 = a^2 b^2 \tag{1}$$

In the work described here, as analysis of contact stresses and areas was being carried out, which are extremely sensitive to geometry, an actual apple form was generated using laser scanning.

## ULTRASONIC MEASUREMENTS

When a wave of ultrasound is incident on an incomplete interface between two materials it will be partially reflected (as shown in Figure 4). The proportion of the amplitude of the incident wave that is reflected is known as the reflection coefficient, *R*.

It has been shown that the reflection coefficient can be defined in terms of the interfacial stiffness, *K*, using a spring model of the interface (where the materials in contact are similar) [19]:

$$|R| = \frac{1}{\sqrt{1+\left(2K/\omega z\right)^2}} \tag{2}$$

where $\omega$ is the angular frequency (= $2\pi f$) of the ultrasound wave and $z$ is the acoustic impedance (the product of the wave speed and density). Tests at low pressures using typical machined surfaces showed that the contact pressure is proportional to the interfacial stiffness [20]. This means a simple calibration can be carried out to relate the two parameters.

## Ultrasonic Apparatus

A spherical focusing 10MHz transducer was mounted in a water bath such that the ultrasonic wave was focused at the apple interface. Ultrasonic waves were generated and received by an ultrasonic pulse-receiver (UPR). The reflected signals were captured on a digital oscilloscope and passed to a PC for processing. A schematic illustrating the set-up of the equipment is shown in Figure 5.

The transducer was positioned using an *x*, *y* stepper controlled by the PC. This enabled ultrasonic readings to be taken using the transducer over an area at prescribed intervals (i.e. a C-scan). The dimensions and resolution of the scan could be varied and selected according to specimen geometry and the accuracy required. Focusing height adjustment of the transducer was achieved manually.

## Apple Specimens and Experimental Parameters

'Golden Delicious' apples were used for the tests. This variety was chosen because it has a pale skin, which means any discolouration due to bruising is more evident. Sugar content and firmness tests were carried out on the apples prior to distribution, which enabled apples with consistent properties to be used in the tests. A purpose built spherometer was also used to measure the radius of curvature of the apples to enable Hertz predictions of the contact area and peak stresses to be calculated.

Loads used in the tests ranged from 2N to 100N. These are typical of loads experienced by apples in bulk storage bins [1]. Apple deflections at each of the loads were recorded.

## Scanning procedure

An apple was placed in the loading apparatus, as shown in Figure 6. A compressed spring arrangement was used to load the apple against a perspex counterface. Perspex was used as it has a similar acoustic impedance to that of the apple ($z = \rho c$, where $\rho$ is the density of the material and $c$ is the speed of sound in the material) ($z$ is 0.18 for perspex and 0.15 for water [21]), which improves the quality of the ultrasonic measurements and is typical of materials used to manufacture apple storage bins. The transducer height was then set to scan the apple/perspex contact. The ultrasonic wave is refracted at the water/perspex interface. The height of the transducer required to focus the wave on the interface was calculated using Snell's law of refraction [22]. A scan was then taken of the contact area. The load was then increased and another scan taken, until the full range of loads to be tested were complete.

A reference measurement was taken at a point away from the contact to determine the proportion of the ultrasonic signal lost due to attenuation in the perspex. The reflected pulses from the apple/perspex contact were then divided by the reference recording to obtain reflection coefficients.

**Calibration**

In previous studies, the calibration of reflection coefficient to interfacial stiffness has been carried out using simple specimens of known contact area, made from the same materials as the components under investigation [12, 13]. With apples, however, this was impossible. In this case a different approach was used.

The total applied load ($P$) is equal to the sum of the pressure for each *cell* ($p$) in the scan multiplied by the area of the cell (d$A$):

$$P = \sum p\mathrm{d}A \tag{3}$$

The contact pressure was assumed to be proportional to the stiffness ($K$) (where c is the constant of proportionality) giving:

$$P = \mathrm{c}\sum K\mathrm{d}A \tag{4}$$

The applied load for each scan, $P$, was known and the total stiffness was determined from the reflection coefficient values using the spring model (Equation 1). The constant c was then calculated for each scan for the first apple. It was found that c was very similar for each scan proving that $K$ is proportional to $p$ for this case. Values of c were found to be very similar for the subsequent apples so the value determined for the first apple was used for all calibrations.

## Results

Examples of ultrasonic scans are shown in Figure 7. As would be expected, the contact area increases with load applied. In all scans, the maximum pressure is at the centre of the contact, and the pressure falls away towards the edge. The maximum stress in the contact remains at a level of around 0.5MPa for all loads. The area of the contact at this peak value, however, rises as the load is increased. This suggests that the apple flesh reaches its *failure* or *yield* point at this stress.

It was interesting to note that the damage caused in the ultrasonic testing, while resulting in a *dent* on the apple surface, did not lead to any discolouration. This is nothing new, but is not often reported. Peeling back the skin revealed that some browning of the flesh was evident, the area of which was much smaller than that of the dent. The significance of this will be discussed further on.

Figure 8 shows contact area against load for four different 'Golden Delicious' apple specimens. Results are relatively similar for each specimen, despite the slight variations in geometry. The industry visible bruise threshold of 100mm$^2$ is also shown. The results shown indicate that at loads above around 35N, the contact area will be over this threshold (although as noted above the area of discolouration is smaller and so would go through the threshold at a higher load).

Also shown on the plots are the Hertz approximations for contact area. These were calculated assuming an elliptical contact (for equations see reference [23]) with the values of radii of curvature measured using a spherometer (these were typically in the range 30 – 50mm, an average was used in the calculations).

The Hertz predictions compare quite well with the ultrasonic results. However, the peak stresses predicted by Hertz analysis are of the order of 2-3 MPa, which is well above that determined by ultrasonic measurements. Hertz analysis is only valid for elastic contacts though, which would explain this discrepancy.

As mentioned earlier, bioyield points for apple flesh have been observed (for ‘Jonica’ apples) at loads of approximately 40N and 100N [8]. In terms of the data collected here, it would be expected that at a bioyield point the contact area would be larger and that the proportion of the contact at the yield stress would increase significantly. If the results for specimen 4 are isolated and the proportion of the contact at the yield stress (0.5MPa) is plotted (as shown in Figure 9), it is possible to see such increases at loads around the values measured previously.

The proportion of the area at the yield stress indicates that the ‘bruise’ area should be a lot lower than that of the contact area if it is assumed that apple flesh above yield will be damaged enough to discolour. This was seen after peeling back the skin on the apples tested here and has been noted before in previous investigations of dynamic apple-to-apple contacts [24, 25]. For apple specimen 4, just considering the area of contact at yield would bring the threshold load up to around 80N, so clearly using the contact area would give a very conservative estimate. It is likely that the real bruise area will be somewhere between the contact area and the area of the contact at yield.

## FINITE ELEMENT ANALYSIS

### Mesh Construction

In order to use the geometry of an actual apple in the FE modelling, a laser scan was created of a ‘Golden Delicious’ apple, which was then imported into ANSYS LS-DYNA software (Version 8) to create a mesh. The apple used for scanning is shown in Figure 10a. The apple was sprayed its magnaflux spot check SKD-S2 developer to provide a reflective surface for the laser scanner. The geometry of a real apple is complex and non-symmetrical so the volume was free meshed with tetrahedral elements, as shown in Figure 10b. It was found that a density of 17000 elements was sufficient to accurately represent the apple geometry and also allowed the model to be solved with the resources available.

To simplify the modelling, isotropic properties were assumed, as they have been in most previous FE studies of apples [14, 15]. A Young's modulus of 4MPa was used, as determined for 'Golden Delicious' flesh in the appropriate region of the apple by Abbot & Lu [16]. The data in Table 2 illustrates how the Young's Modulus actually varies between the various parts of an apple. Abbott & Lu [16] have also shown that the properties of apple flesh vary in different parts of the apple and are different if loading is applied from varying directions.

Linear elastic material properties were also assumed, and while this is probably not valid for apple flesh, this is how it has been modelled in previous work [14, 15], so as a first attempt it was thought reasonable. A sensitivity analysis could be carried out on the flesh properties to ascertain their influence on the results, but was not done as part of this work.

To replicate the loading in the ultrasonic apparatus, the apple was placed between two plates (the top plate with the properties of Perspex and the bottom those of steel). The bottom plate was fixed and the top plate was displaced to achieve the desired normal load on the apple, as shown in Figure 11. Loads of 30, 50, 80 and 100N were applied and contact areas and maximum contact pressures determined.

## Results

The results of the FE modelling are shown in Table 3. The contact pressure from FE analysis for an apple/perspex contact at 100N is shown in Figure 12. As can be seen the spread on contact pressure is not uniform. This may be because an actual apple geometry has been used and the surface waviness has caused the interface pressure to be fragmented at this load. The maximum contact pressure is about 0.65MPa, which is slightly higher than the value determined in the ultrasonic testing, also, as shown in Table 3, the maximum stress continues to increase as the load is increased. This is because of the assumptions made regarding the properties of the apple flesh, such as linear elastic and isotropic properties, but it is not clear to what degree. Figure 13 illustrates how the contact evolves as load is increased.

## DISCUSSION

### Contact Areas and Pressures

The ultrasonic scans showed that the contact pressure was highest at the centre of all the contacts, falling away towards the edge (as shown in Figure 7). This differs from those of previous investigations. Measurements carried out by Herold et al. [9] using a commercial tactile sensing system showed that up to a certain load this was the case, but above the greatest pressure was at the edge of the contact. This critical load was thought to correspond to the bioyield point [17]. There are obvious differences between the two techniques, the commercial tactile system is invasive and could not be calibrated accurately, and of course, different apples were used (‘Jonica’ apples), which will have different yield points.

It was clear in the ultrasonic scans that the maximum contact pressure was not increasing with applied load. This implies that the maximum value determined was that at which the apple flesh was yielding. The value of peak pressure observed, was 0.5MPa. This fits in well with measurements of ‘Golden Delicious’ apple flesh failure stress recorded by Abbott & Lu [16] of 0.40-0.51MPa.

Analysis of the proportion of the contact area at the failure stress at each load revealed that possible bioyield points could be identified (see Figure 9). The points identified correspond to those found in previous work [7].

Contact areas increased with applied load (as shown in Figures 7 and 8). The threshold load of 35N for damage above 100mm$^2$ (the industry standard), may be conservative. Contact areas are likely to be larger than bruise areas, but as yet no relationship has been determined. Previous work on apple-to-apple contacts [24, 25] has shown that measured surface areas may be up to 25% higher than the actual bruise area. In this work, the level of damage is probably better reflected by the area at peak contact pressure. This area also increased with applied load, but did not reach 100mm$^2$ until the load was over 80N (see Figure 9).

Comparing the contact areas for the ultrasonic measurements and FE, there is quite good correlation (as shown in Figure 14). This is despite the fact it is unlikely that apples used in ultrasonic measurements had the same values of mechanical properties as those used in the finite element modelling and they certainly did not have exactly the same geometry.

Peak stresses were also of the same order of magnitude at 0.4-0.7MPa for the FE and 0.5MPa for the ultrasound. However, the values for FE increased with rising loads because of the assumption of linear elastic material properties. The results, however, give a measure of validation for the FE model, despite its inadequacies. Clearly it can be improved by introducing elastic-plastic properties and by modelling the skin and core as separate entities to the flesh and perhaps by actually modelling the cells that make up the apple flesh.

In its present form, however, it could still prove a useful tool in assessing the effect of packaging media on contact stresses and help in designing packaging to reduce the likelihood of bruising occurring.

**Apple Bruising**

No discolouration was seen in the bruises on the test apples (this may have been because insufficient aging time was allowed – quite often discolouration does not occur until 24 hours after the loading event). This suggests that, although the apple flesh cells were crushed, this did not lead to breaking of the cell walls. Work on visual inspection of fruit by buyers [26] suggests that size of damage is not the most important factor, and that the visual impact of the fruit is more influential. This implies that if damage is present, but not immediately obvious, then the buyer's decision will not be affected. If, therefore bruises are unlikely to occur at the static loads encountered in a bulk bin, then this may not be a problem. There must be a threshold size, however, over which the buyer will discard an apple regardless of whether discolouration is obvious or not.

A strong correlation has been observed between bruise volume and energy absorbed for both dynamic impact loading and quasi-static loading (continuous load increase at very low velocity) of 'Granny Smith' apples [5]. This work concluded that apple flesh more easily bruised by slow compression, for the same applied energy.

Energy applied in the static tests carried out in this work was calculated from the deflection data measured during testing. A typical force deflection plot is shown in Figure 15. The energy is simply the area under the curve. The contact areas were then plotted against energy and compared with bruise areas from dynamic (drop) tests also carried out with 'Golden Delicious' apples [27] (see Figure 16). A high speed video camera was used in the dynamic testing to allow apple velocity before and after impact to be determined in order to calculate the energy absorbed during the impact. Typically bruise volume is plotted against energy, but as it is the area that a consumer will see, in this case bruise area was used.

As can be seen, in this work dynamic, rather than statically loaded apples, exhibited larger bruise areas (bruise volumes were also higher). It should be noted that the dynamic measurements were of actual bruises not contact areas so the difference between static and dynamic in terms of bruise area is probably larger.

As mentioned above, a relationship between contact area and bruise area has yet to be determined in this work. It could be that the static bruises are actually larger, but calculation of bruise volume for the statically loaded apples was inhibited by the lack of discolouration seen. This in itself is quite revealing as it indicates that the cell walls may not been breached and the contained enzymes that, when mixed, cause the discolouration, are still being separated.

In the work of Holt [5] the cell walls had clearly been broken down. This may have been due to slight differences in the type of loading used and the fact that a different apple type was used ('Granny Smith'). Apples were loaded quasi-statically in a hydraulic test machine, i.e. the loading was increased continuously to the maximum rather than the very slow incremental approach used here, where apples remained at each load for a long time, while ultrasonic scanning was carried out. The slower incremental approach is perhaps, however, more representative of the type of loading experienced by apples in storage, where loads will increase very gradually as more apples are added to a storage bin, for example.

Holt [5] hypothesised that the two different failure mechanisms identified for cellulose micro fibrils in the apple cell walls identified previously [24] resulted in the different bruise volumes found for dynamic and quasi-static loading. It was reported that the microfibrils can fail by straightening out and slipping relative to each other or by straightening out and breaking [28]. Holt [5] postulated that under quasi-static loading the fibrils will straighten and slip and for dynamic loading will straighten and snap, much like a slack rope might when suddenly loaded. This suggests that the failure process may be linked to the rate of energy application rather than the amount of energy and in that case bruising should be higher for the dynamic case. The slipping may not necessarily lead to failure, which could explain the lack of discolouration seen in the static tests reported here and the smaller resultant bruises. Clearly, given the apparent lack of clarity, there is a need to do some more complex studies, perhaps FE analysis of the apple flesh structure at a cellular level to gain an improved understanding of what is actually happening. Some work has been carried out in this area using an imaging technique for predicting individual cell damage and bruise volumes [29].

## CONCLUSIONS

A novel ultrasonic technique has been used to characterise areas and pressures in apple to perspex contacts. Results differ from those using an invasive commercial tactile system, where peak stresses were seen to migrate from the centre of the contact to the edge above a critical load. The failure stresses determined in the ultrasonic results, however, compare well with previous measurements and this, combined with knowledge of the behaviour of more conventional sphere on flat contacts predicted by elastic contact theory, suggests that they appear more reliable.

To back this up the ultrasonic results compare well with those from finite element modelling using a mesh generated using an actual apple geometry generated by a laser scan. This model has a number of simplifications, including isotropic properties, and therefore could be improved by considering the skin and core to be separate entities to the flesh and assigning more realistic properties to these parts or by modelling the actual cells that make up the apple flesh. It is clear though that the model presented here still has the potential to be used a design tool for assessing packaging material and designs to help reduce the likelihood of damage occurring.

A load of 35N was identified above which the contact area was higher than 100mm$^2$, which is the industry standard for discarding apples. This was thought to be conservative, however, as actual damage is not likely to be equal to the area of contact. A threshold would be better defined as the area at the peak pressure (flesh failure stress) within the contact, which did not reach 100mm$^2$ until a load over 80N is applied.

## REFERENCES


1. A.F. Bollen, E.J. Timm, B.T. Dela Rue, Relation of individual forces on apples and bruising during orchard transport of bulk bins, Applied Engineering in Agriculture 17(2) (2001a), 193-200.
2. I. Peggie, Technical problems in the retail marketing of fruit and vegetables, Proceedings of Fifth Australian Fruit and Vegetable Storage Conference (1968, 142-155.
3. J.B. O'Loughlin. The bruising of fruit during transport and storage, Proceedings of the Fourth Australian Fruit and Vegetable Storage Conference (1964), 1-13.
4. J.M. Labavitch, L.C. Greve, E. Mitcham, Fruit bruising: it's more than skin deep, Perishables Handling Quarterly, 95 (1998), 7-9.
5. D.W. Pang, C.J. Studman, N.H. Banks, Apple bruising thresholds for an instrumented sphere, Transactions of the ASAE, 37(3) (1994), 893-897.
6. A.F. Bollen, N.R. Cox, B.T. Dela Rue, D.J. Painter, A descriptor for damage susceptibility of a population of produce, Journal of Agricultural Engineering Research, 78(4) (2001b), 391-395.
7. J.E. Holt, D. Schoorl, Bruising and energy dissipation in apples, Journal of Textures Studies, 7 (1977), 421-432.
8. J.L. Garcia, M. Ruiz-Altisent, P. Barreiro, Factors influencing mechanical properties and bruise susceptibility of apples and pears, Journal of Agricultural Engineering Research, 61 (1995), 11-18.
9. B. Herold, M. Geyer, C.J. Studman, Fruit contact pressure distributions – equipment, Computers and Electronics in Agriculture 32 (2001), 167-179.
10. G.F. Rabelo, I.M. Fabbro, A.W. Linares, Contact stress area measurement of spherical fruit, Proceedings of Sensors in Horticulture III (2001), 195-200.

11. R.S. Dwyer-Joyce, B.W. Drinkwater, Analysis of contact pressure using ultrasonic reflection, Proceedings of 11th Annual Conference on Experimental Mechanics, Balkema, Rotterdam (1998), 747-754.

12. K. Hodgson, R.S. Dwyer-Joyce, B.W. Drinkwater, Ultrasound as an experimental tool for investigating engineering contacts. Proceedings of the 9th Nordic Symposium on Tribology, 'Nordic 2000', Eds. Andersson P; Ronkainen H; Holmberg K, 2 (2000), 377-386.

13. M.B. Marshall, R. Lewis, B.W. Drinkwater, R.S. Dwyer-Joyce, An ultrasonic approach for contact stress mapping in joints and concentrated contacts, Journal of Strain Analysis for Engineering Design, 39(4) (2004), 339-350.

14. R. Lu, J.A. Abbott, Finite element analysis of modes of vibration in apples, Journal of Texture Studies, 27 (1996), 265-286.

15. R. Lu, J.A. Abbott, Finite element modelling of transient responses of apples to impulse excitation, Transactions of the ASAE, 40(5) (1997), 395-1409.

16. J.A. Abbott, R. Lu, Anisotropic mechanical properties of apples, Transactions of the ASAE 39(4) (1996), 1451-1459.

17. N.N. Mohsenin, Physical properties of plant and animal materials, Vol. 1, Gordon and Breach Publishers, New York (1970).

18. S. Moustafa, B.A. Stout, A mathematical model for the apple fruit, Michigan Agri. Exp. Station Quart. Bull. 49(4) (1967), 450-458

19. K. Kendall, D. Tabor, An ultrasonic study of the area of contact between stationary and sliding surfaces, Proceedings of the Royal Society, Series A, 323 (1971), 321-340.

20. B.W. Drinkwater, R.S. Dwyer-Joyce, P. Cawley, A study of the interaction between ultrasound and a partially contacting solid-solid interface, Proceedings of the Royal Society, Series A, 452(1955) (1996), 2613-2628.

21. J. Krautkrämer, H. Krautkrämer, Ultrasonic Testing of Materials, Springer Verlag, New York (1990).

22. W.B. Joyce, A. Joyce, Descartes, Newton, and Snell's law, J. Opt. Soc. Amer. 66(1) (1976), 1-8.

23. J.A. Williams, Engineering Tribology, Oxford University Press, Oxford (1994).

24. W. Pang, C.J. Studman, G.T. Ward, Bruising damage in apple-to-apple impact, Journal of Agricultural Engineering Research, 52 (1992), 229-240.

25. C.J. Studman, G.K. Brown, E.J. Timm, N.L. Schulte, M.J. Vreede, Bruising on blush and non-blush sides in apple-to-apple impacts, Transactions of the ASAE, 40(6), 1655-1663.

26. M. Cliff, K. Sanford, W. Wismer, C. Hampson, Use of digital images for evaluation of factors responsible for visual preference of apples by consumers, Hortscience 37(7) (2002), 1127-1131.

27. L.A. Canty, An engineering approach to the study of apple bruising, MEng Thesis, The University of Sheffield (2004).

28. R.D. Preston, Mechanical properties of the cell wall, Handbuch der Pflazenphysiologie 1 (1955), 749.

29 A.-C. Roudot, F. Dupra, C. Wenian, Modelling the response of apples to loads, Journal of Agricultural Engineering Research, 48 (1991), 249-259.

**Figure Captions**

**Figure 1**

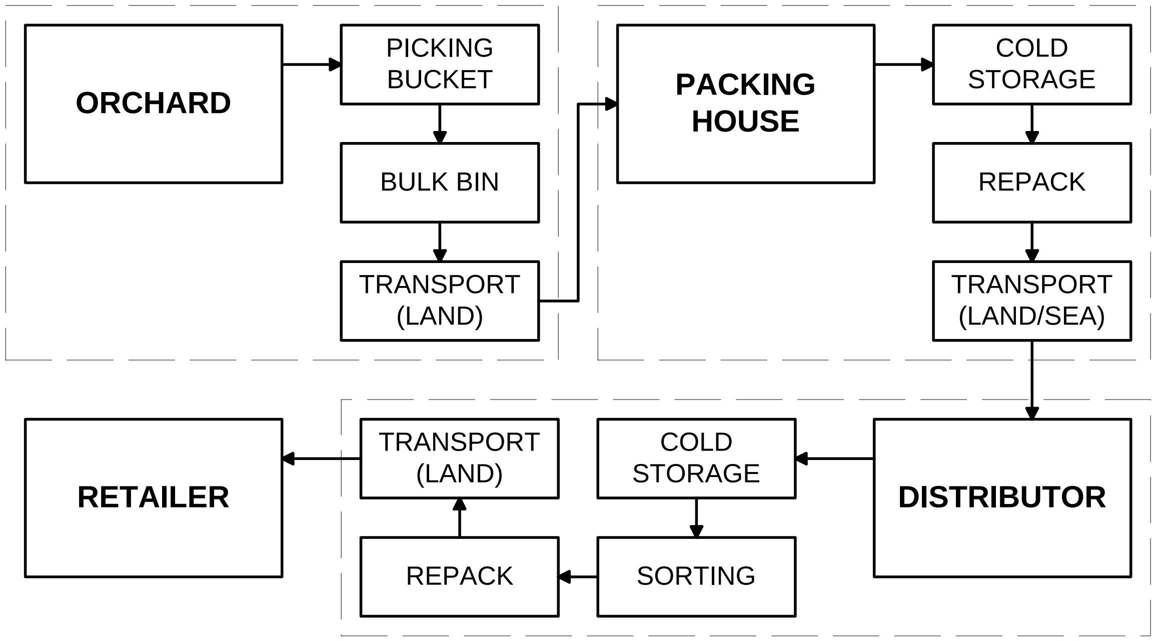


**Figure 2**

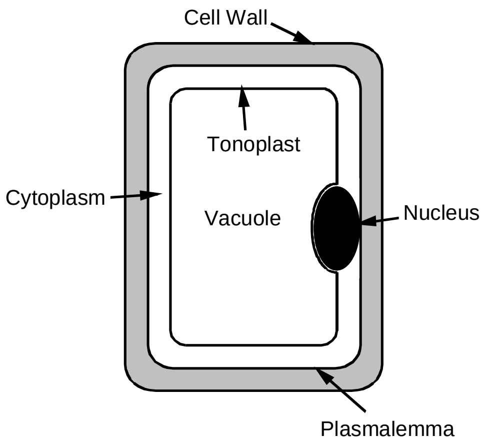

**Figure 3**

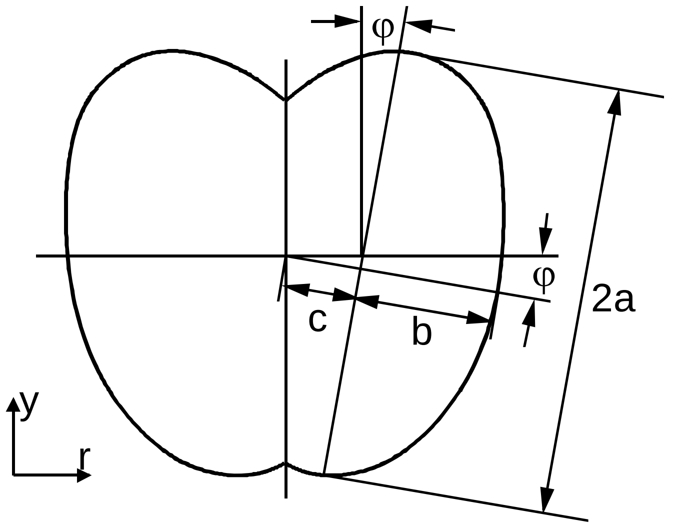

**Figure 4**

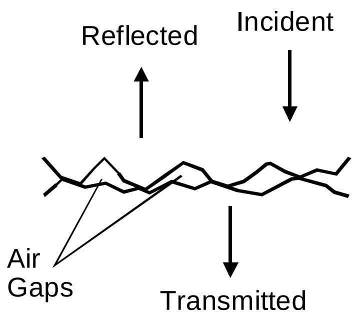


**Figure 5**

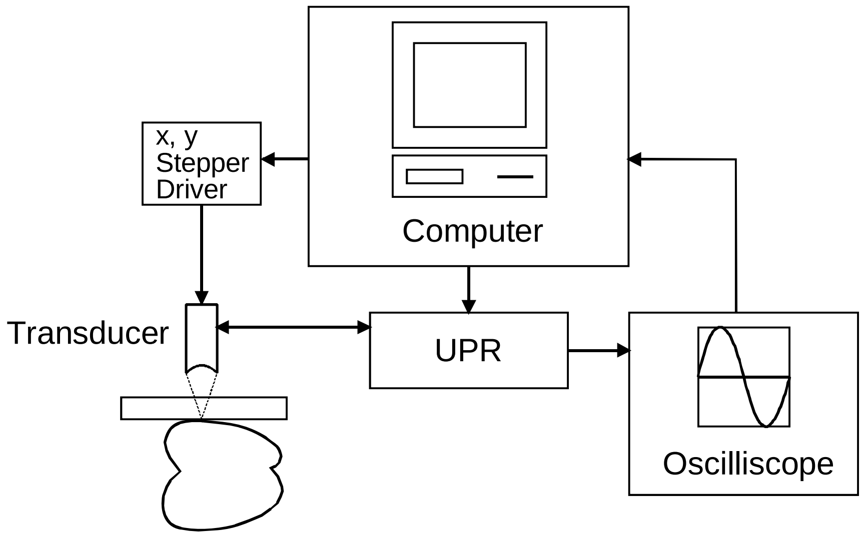

**Figure 6**

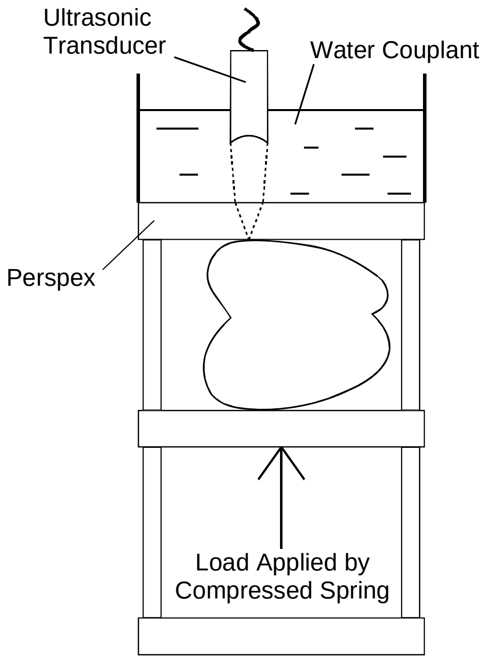
Ultrasonic
Transducer
Water Couplant
Perspex
Load Applied by
Compressed Spring

**Figure 7**

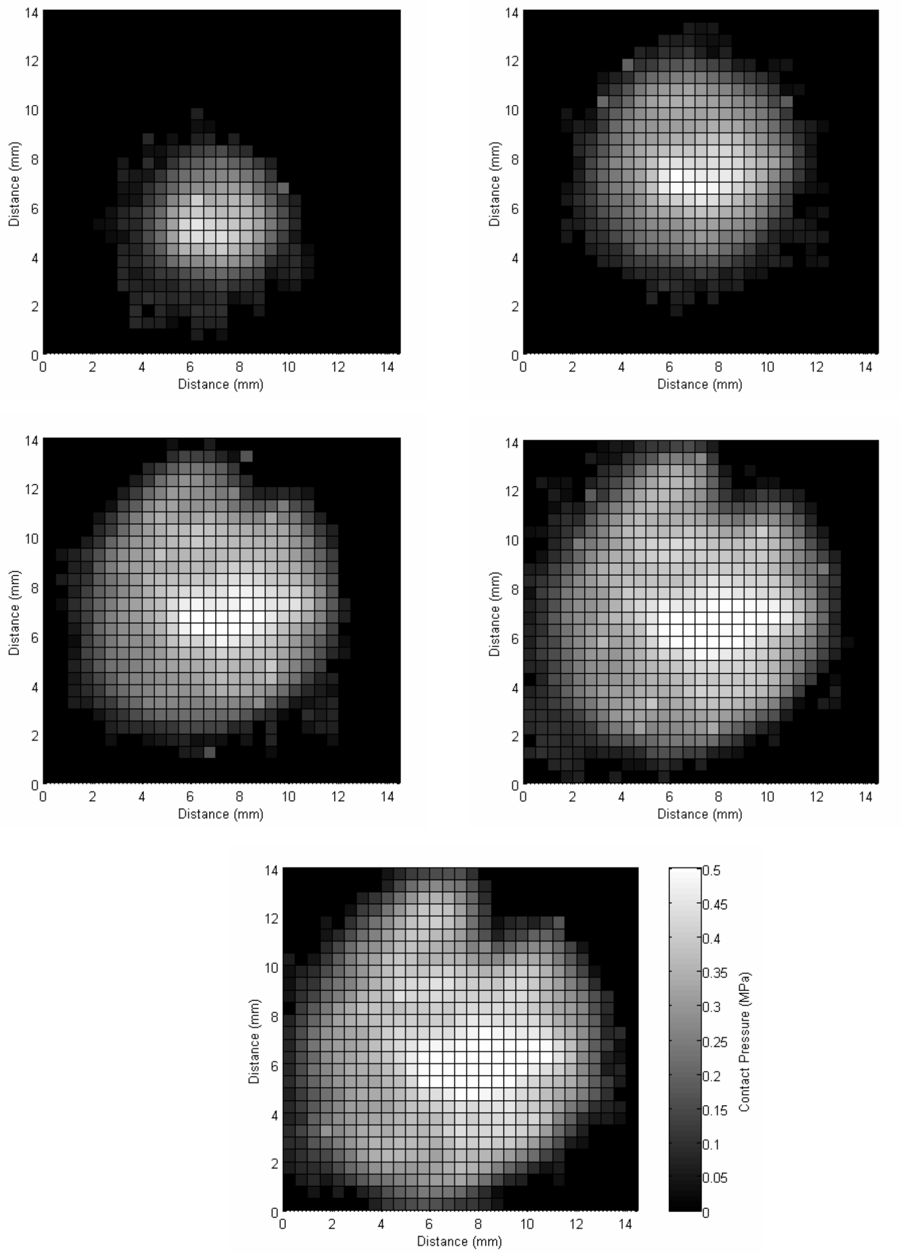
Distance (mm)
Distance (mm)
Contact Pressure (MPa)
0
0.05
0.1
0.15
0.2
0.25
0.3
0.35
0.4
0.45
0.5

**Figure 8**

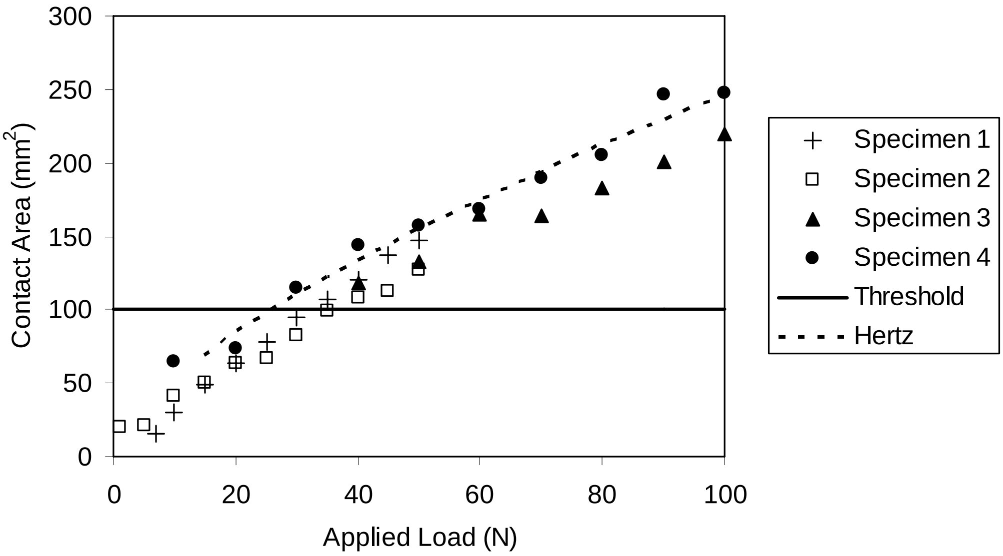


**Figure 9**

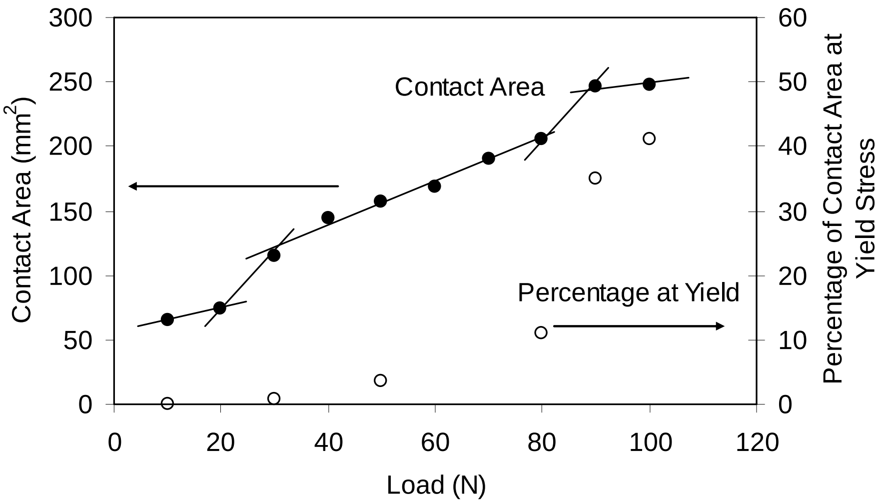

**Figure 10**

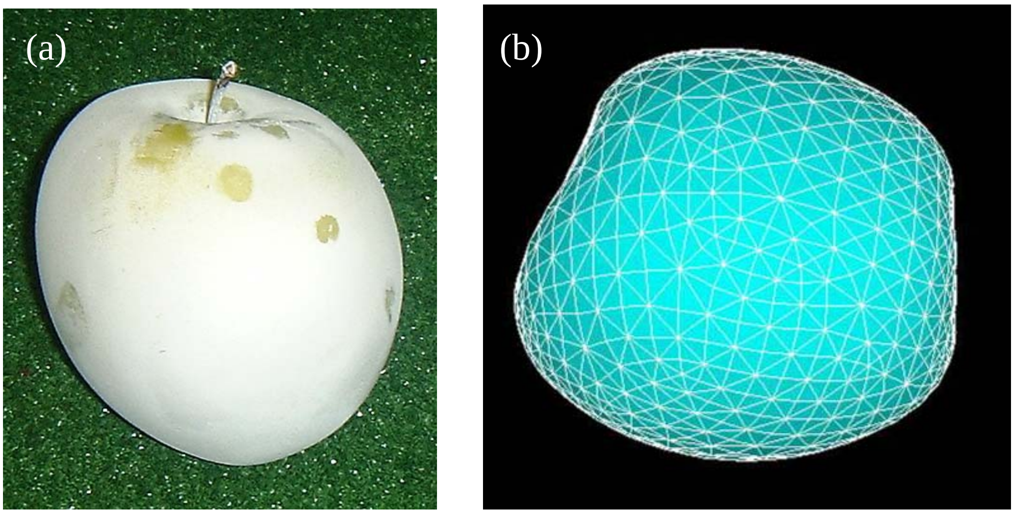


**Figure 11**

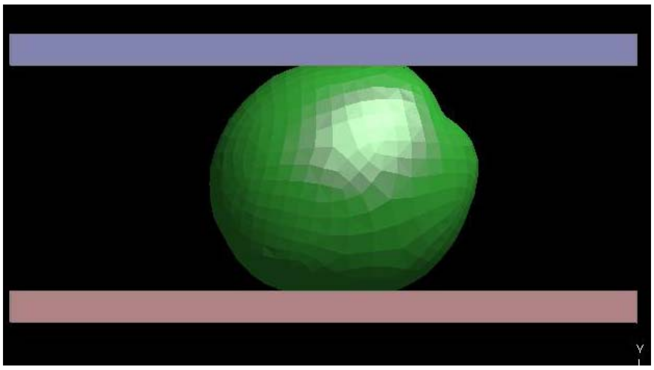

**Figure 12**

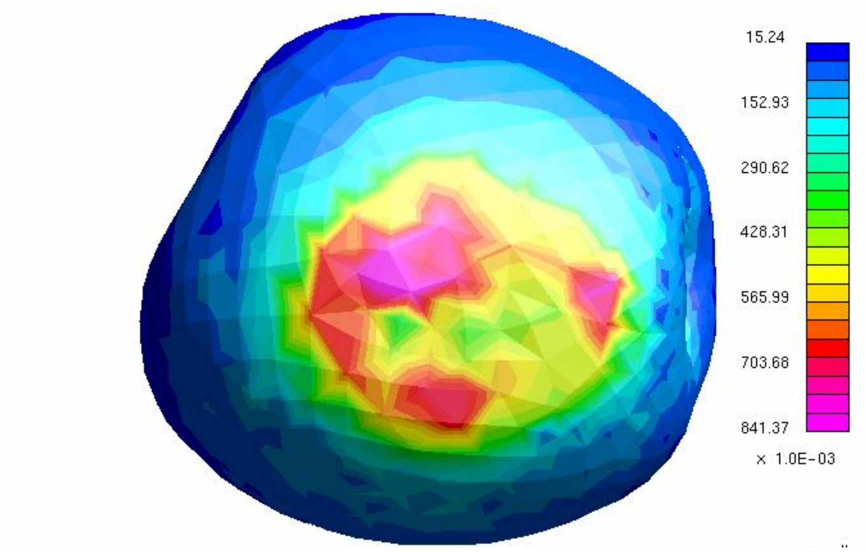


**Figure 13**

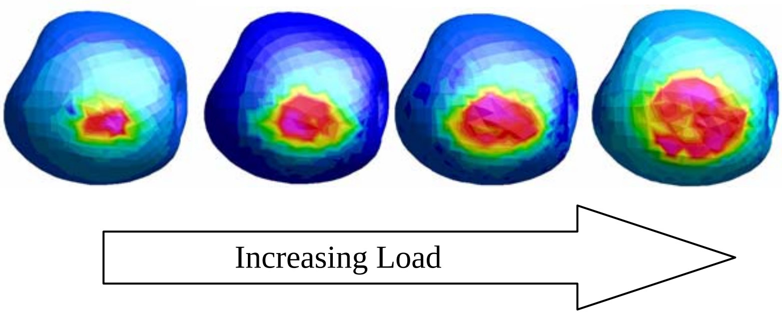

**Figure 14**

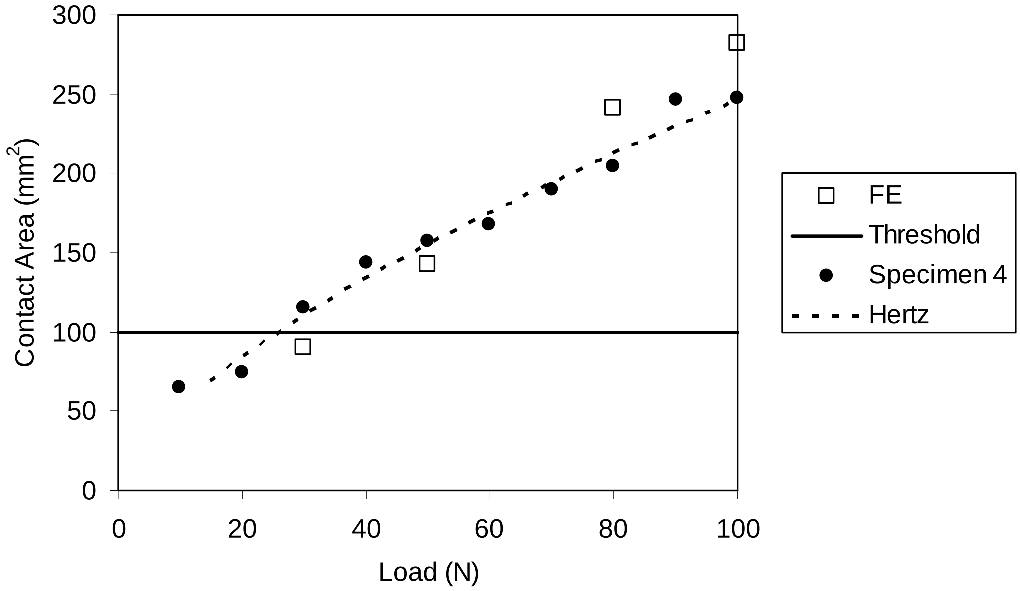


**Figure 15**

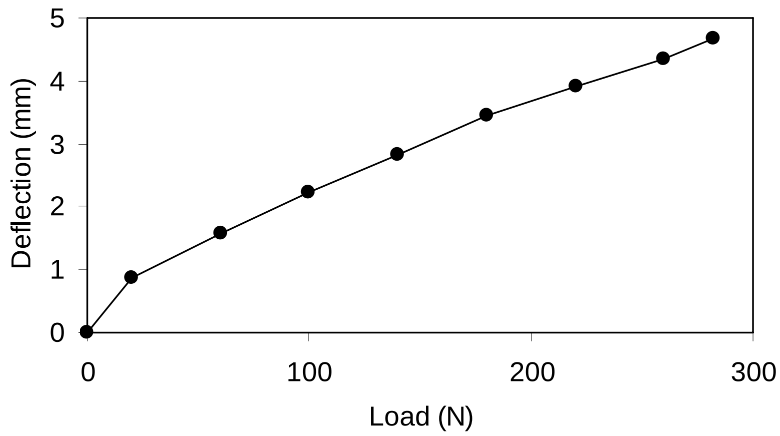

**Figure 16**

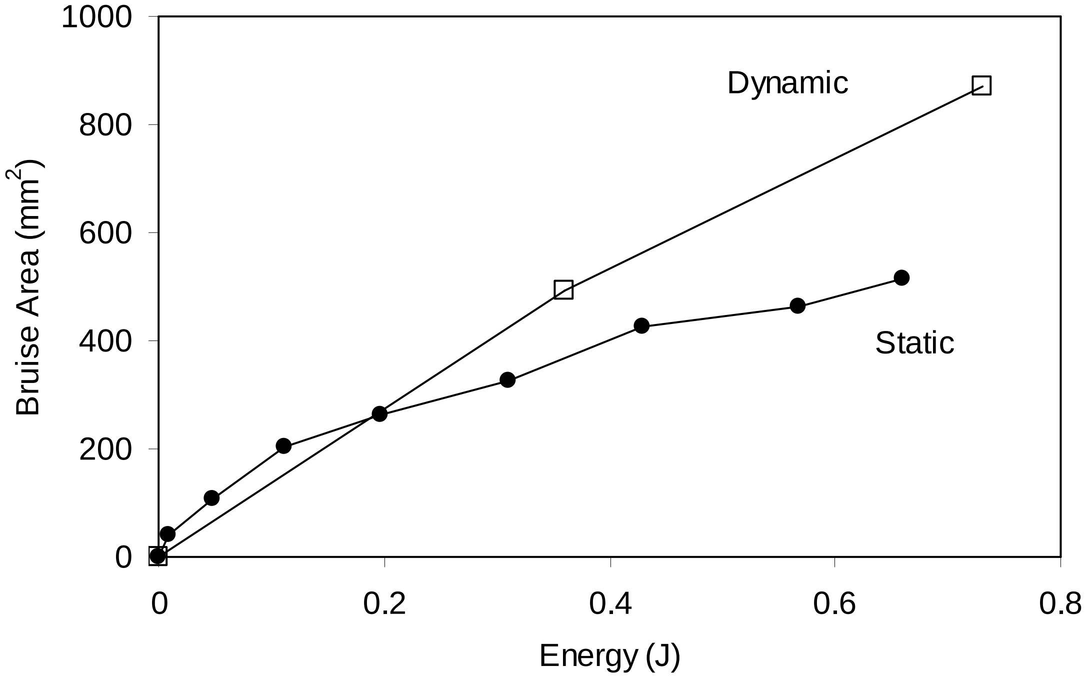

1000
800
600
400
200
0
Bruise Area ($mm^2$)
Dynamic
Static
0
0.2
0.4
0.6
0.8
Energy (J)

**Table Captions**

**Table 1**

| Point in Journey | Process Stage | Type of Loading | Potential Drop Height or Static Load |
|---|---|---|---|
| Orchard | Picking Bucket | Dynamic | 0.6m |
| | Bulk Bin | Dynamic/Static | 0.6m/60N [1] |
| | Transport | Dynamic (vibration)/Static | |
| Packing House | Repack | Dynamic | |
| Distributor | Sorting (conveyors etc.) | Dynamic | 0.05-0.15m |
| Retailer | Putting on Display | Dynamic/Static | 0.05-0.3m |

**Table 2**

| Region of Apple | Skin | Flesh | Core |
|---|---|---|---|
| Young's Modulus (MPa) | 20 | 4 | 8 |
| Failure Stress (MPa) | - | 0.40-0.51 | - |
| Poisson's Ratio | 0.3 | 0.3 | 0.3 |

**Table 3**

| Load (N) | Contact Area ($mm^2$) | Maximum Contact Stress (MPa) |
|---|---|---|
| 30 | 90.1 | 0.32 |
| 50 | 142.2 | 0.42 |
| 80 | 241.7 | 0.52 |
| 100 | 282.34 | 0.65 |